ANN Synthesis Models Trained with Modified GA-LM Algorithm for ACPWs with Conductor Backing and Substrate Overlaying

Zhongbao Wang, Shaojun Fang, and Shiqiang Fu

Accurate synthesis models based on artificial neural networks (ANNs) are proposed to directly obtain the physical dimensions of an asymmetric coplanar waveguide with conductor backing and substrate overlaying (ACPWCBSO). First, the ACPWCBSO is analyzed with the conformal mapping technique (CMT) to obtain the training data. Then, a modified genetic-algorithm-Levenberg-Marquardt (GA-LM) algorithm is adopted to train ANNs. In the algorithm, the maximal relative error (MRE) is used as the fitness function of the chromosomes to guarantee that the MRE is small, while the mean square error is used as the error function in LM training to ensure that the average relative error is small. The MRE of ANNs trained with the modified GA-LM algorithm is less than 8.1%, which is smaller than those trained with the existing GA-LM algorithm and the LM algorithm (greater than 15%). Lastly, the ANN synthesis models are validated by the CMT analysis, electromagnetic simulation, and measurements.

Keywords: ACPWs, synthesis models, ANN, CMT, modified GA-LM algorithm.

Manuscript received Feb. 5, 2012; revised May 13, 2012; accepted June 1, 2012.

This work was supported jointly by the National Natural Science Foundation of China (No. 61071044), the Traffic Applied Basic Research Project of the Ministry of Transport of China (No. 2010-329-225-030), the Fundamental Research Funds for the Central Universities (No. 2012TD007) and the National Key Technologies R&D Program of China (No. 2012BAH36B01).

Zhongbao Wang (phone: +86 411 84729279, wangzb@dlmu.edu.cn), Shaojun Fang (fangshj@dlmu.edu.cn), and Shiqiang Fu (fushq@dlmu.edu.cn) are with the School of Information Science and Technology, Dalian Maritime University, Liaoning, China.

http://dx.doi.org/10.4218/etrij.12.0112.0088

I. Introduction

Coplanar waveguides (CPWs) are widely adopted in many microwave circuits [1] and antennas [2], [3]. Asymmetric coplanar waveguides (ACPWs) provide additional degrees of freedom to control the line characteristic and to optimize the circuit layout. However, the conventional ACPW [4] is sensitive to environmental effects because its fields are less confined than those of microstrip lines. To solve this problem, an ACPW with conductor backing (ACPWCB) was proposed in [5]. It allows easy implementation of mixed coplanar-microstrip circuits and reduces radiation effects. Similar to microstrip lines, even- and odd-mode phase velocities of coupled CPWs are unequal as a result of poor isolation for coupled-line directional couplers [6]. Many methods have been presented to overcome this shortcoming, among which substrate overlaying [7] not only improves the isolation but also provides a protective layer for circuits. In [8], ACPWs with conductor backing and substrate overlaying (ACPWCBSO) were adopted in designing the feed network for patch antennas, and the overlaying substrate can function as the substrate for the patch antennas, which means that the patch antennas can be easily integrated with the feed network.

Currently, some ACPWs have been analyzed with the conformal mapping technique (CMT) [4], [5], [9]-[12]. In 1995, the overlaid supported ACPW [10] was analyzed with the CMT. In [11], the analysis formulas were presented for calculating the quasi-static parameters of the ACPWCB, ACPW with upper shielding, and ACPWCB with upper shielding. The effective permittivity, characteristic impedance,

and electric-field strength of the ACPWCB have been determined in [12]. However, the CMT analysis formulas [4], [5], [9]-[12] are too complicated to understand, and there are some typographical errors in [10] and [11]. Owing to the increasing popularity of ACPWs for the design of microwave circuits, it becomes highly desirable to have accurate computer-aided design (CAD) models for directly obtaining the physical dimensions of ACPWs. Based on the data obtained from the CTM analysis, the synthesis formulas for the ACPW and the ACPWCB had been developed with differential evolution (DE) and particle swarm optimization (PSO) algorithms [13], [14]. However, the synthesis formulas cannot be used for symmetric CPWs. Furthermore, to the best of our knowledge, there is no CAD model for the synthesis of the ACPWCBSO and the ACPWs with upper shielding.

The ANN has recently gained attention as a fast and flexible vehicle for microwave modeling, simulation, and optimization [15]-[17]. The success of ANNs in terms of a particular problem depends on the adequacy of the training algorithm. The existing gradient-based techniques, such as the back propagation (BP) and the Levenberg-Marquardt (LM) algorithms, had been used to train ANNs for constructing the analysis and synthesis models of various microwave transmission lines [18]-[20]. However, as these algorithms perform local searches, they are susceptible to the local minimum problem. A stochastic algorithm [21], such as the genetic algorithm (GA) or the simulated annealing (SA), is an interesting alternative for ANN training, since it is less sensitive to local minima. Nevertheless, such algorithms are generally slower than the faster versions of gradient-based techniques [16]. A promising approach is the hybrid training that combines the advantages of both stochastic algorithms and gradient-based techniques. In 1990, Belew and others [22] combined the GA with the BP, obtaining better results than using either algorithm in isolation. In 2003, Prudêncio and Ludermir [23] combined the GA and the LM. In 2007, Kim and others [24] combined the PSO and gradient descent algorithms. For various training algorithms, the training processes are carried out by iteratively adjusting the connection weights to minimize an error function. The mean square error (MSE) is usually used as the error function. However, even with small MSE, the maximal relative error (MRE) of the ANNs is not guaranteed to be small. As a result, the MRE of the ANNs trained with the existing algorithms, such as the GA-LM hybrid algorithm [23], [25] and the LM algorithm [26], may be greater than 15%. Therefore, some results obtained from ANN models [18]-[20] are inaccurate. To obtain accurate ANN synthesis models for the ACPWCBSO, the GA-LM algorithm [23], [25] will be modified in section III and adopted to train ANNs. In the modified GA-LM algorithm, both MRE and MSE will be taken into account.

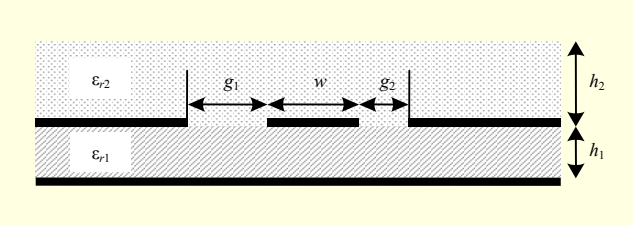

Fig. 1. Cross-section of ACPWCBSO.

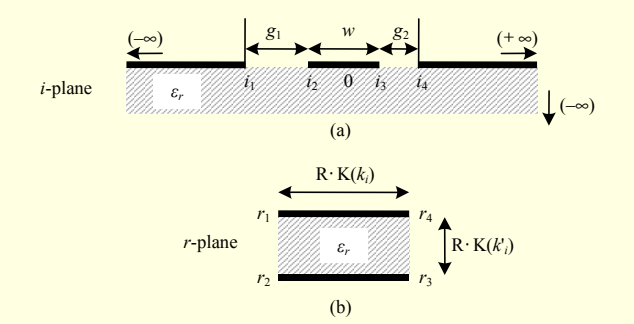

Fig. 2. Conformal mapping for calculating capacitance of ACPW in infinite substrate region: (a) ACPW geometry in i-plane and (b) mapping the lower half-plane of ACPW into parallel-plate capacitor in r-plane.

II. CMT Analysis of ACPWCBSO

To obtain the training data, the CMT is used to analyze the ACPWCBSO. The cross-section of an ACPWCBSO is shown in Fig. 1. In this figure, w represents the central strip width; g_1 and g_2 represent the slot widths. The dielectric substrates have thicknesses of h_1 and h_2 with relative permittivity ε_{r1} and ε_{r2}, respectively. If the dielectric interfaces in the slots are modeled as magnetic walls and all the conductors are assumed to be infinitely thin and perfectly conductive, the overall capacitance per unit length of ACPWCBSO can be written as

$$C = C_0 + C_1 + C_2, \tag{1}$$

where C_0 is the air-space capacitance after removing the dielectric substrates and C_1 is introduced by a dielectric substrate of thickness h_1 with the equivalent relative permittivity (ε_{r1}–1). Similarly, C_2 is related to the dielectric substrate of thickness h_2 with the equivalent relative permittivity (ε_{r2}–1).

1. Capacitance of ACPW in Infinite Substrate Region

As shown in Fig. 2, the lower half-plane is transformed into the rectangular region in the r-plane by the Schwartz-Christoffel transformation [9]-[12]

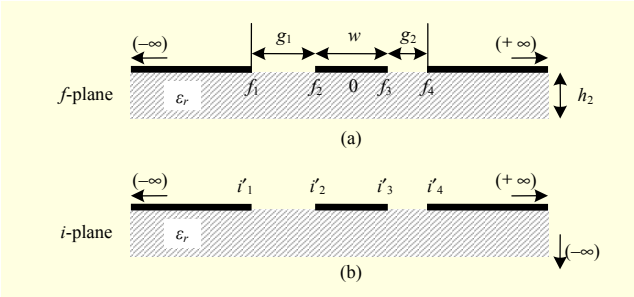

Fig. 3. Conformal mappings for calculating capacitance of ACPW in finite substrate region: (a) ACPW geometry in *f*-plane and (b) mapping finite substrate region into infinite substrate region in *i*-plane.

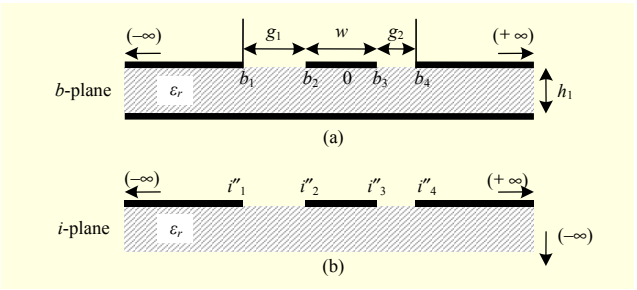

Fig. 4. Conformal mappings for calculating capacitance between ACPW and lower ground plane: (a) CBACPW geometry in *b*-plane and (b) mapping substrate region between ACPW and lower ground plane into infinite substrate region in *i*-plane.

$$r = \int_{i_1}^{i} \frac{di}{\sqrt{(i-i_1)(i-i_2)(i-i_3)(i-i_4)}} . \tag{2}$$

As a result, the capacitance per unit length of the ACPW in the infinite substrate region is

$$C_i = \varepsilon_r \varepsilon_0 \frac{\mathrm{K}(k_i)}{\mathrm{K}(k_i')}, \tag{3}$$

where $\mathrm{K}(k_i)$ represents the complete elliptical integrals of the first kind with the module k_i and

$$k_i' = \sqrt{1-(k_i)^2}\ , \quad k_i = \sqrt{\frac{(i_3-i_2)(i_4-i_1)}{(i_3-i_1)(i_4-i_2)}}\ ,$$

$$i_1 = -\left(\frac{2g_1+w}{2}\right),\ i_2 = -\frac{w}{2},\ i_3 = \frac{w}{2},\ i_4 = \frac{2g_2+w}{2}.$$

2. Capacitance of ACPW in Finite Substrate Region

To obtain the capacitance per unit length of the ACPW in the finite substrate region, the first step is transforming the finite substrate region into an infinite substrate region, as shown in Fig. 3. The transformation is given by a hyperbolic sine function [4]:

$$i' = \sinh\left(\frac{\pi f}{2h_2}\right). \tag{4}$$

Then, using the Schwartz-Christoffel transformation, the capacitance per unit length of the ACPW in the finite substrate region can be obtained by

$$C_f = \varepsilon_r \varepsilon_0 \frac{\mathrm{K}(k_f)}{\mathrm{K}(k_f')}, \tag{5}$$

where $k_f = \sqrt{\frac{(i_3'-i_2')(i_4'-i_1')}{(i_3'-i_1')(i_4'-i_2')}}$, $i_1' = -\sinh\left(\frac{\pi(2g_1+w)}{4h_2}\right)$,

$$i_2' = -\sinh\left(\frac{\pi w}{4h_2}\right),\ i_3' = \sinh\left(\frac{\pi w}{4h_2}\right),\ i_4' = \sinh\left(\frac{\pi(2g_2+w)}{4h_2}\right).$$

3. Capacitance between ACPW and Lower Ground Plane

As shown in Fig. 4, the substrate region between the ACPW and the lower ground plane is transformed into an infinite substrate region. The transformation is given by an exponential function [5]:

$$i'' = \exp\left(\frac{\pi b}{h_1}\right). \tag{6}$$

Again, using the Schwartz-Christoffel transformation, the capacitance per unit length between the ACPW and the lower ground plane is obtained by

$$C_b = \varepsilon_r \varepsilon_0 \frac{\mathrm{K}(k_b)}{\mathrm{K}(k_b')}, \tag{7}$$

where $k_b = \sqrt{\frac{(i_3''-i_2'')(i_4''-i_1'')}{(i_3''-i_1'')(i_4''-i_2'')}}$, $i_1'' = \exp\left(-\frac{\pi(2g_1+w)}{2h_1}\right)$,

$$i_2'' = \exp\left(-\frac{\pi w}{2h_1}\right),\ i_3'' = \exp\left(\frac{\pi w}{2h_1}\right),\ i_4'' = \exp\left(\frac{\pi(2g_2+w)}{2h_1}\right).$$

4. Quasi-Static Parameters of ACPWCBSO

Based on the aforementioned analysis, the air-space capacitance C_0 is obtained by

$$C_0 = C_{0i} + C_{0b} = \varepsilon_0 \frac{\mathrm{K}(k_i)}{\mathrm{K}(k_i')} + \varepsilon_0 \frac{\mathrm{K}(k_b)}{\mathrm{K}(k_b')}. \tag{8}$$

The substrate capacitance C_1 between the ACPW and the lower ground plane with substrate thickness h_1 and equivalent relative permittivity (ε_{r1}–1) is given by

$$C_1 = C_{1b} = (\varepsilon_{r1}-1)\varepsilon_0 \frac{\mathrm{K}(k_b)}{\mathrm{K}(k_b')}, \tag{9}$$

and the capacitance C_2 introduced by the dielectric substrate of thickness h_2 having the equivalent relative permittivity (ε_{r2}–1)

is written as

$$C_2 = C_{2f} = (\varepsilon_{r2} - 1)\varepsilon_0 \frac{\mathrm{K}(k_f)}{\mathrm{K}(k_f')}. \quad (10)$$

Thus, the overall capacitance of the ACPWCBSO is

$$C = \varepsilon_0 \frac{\mathrm{K}(k_i)}{\mathrm{K}(k_i')} + \varepsilon_{r1}\varepsilon_0 \frac{\mathrm{K}(k_b)}{\mathrm{K}(k_b')} + (\varepsilon_{r2} - 1)\varepsilon_0 \frac{\mathrm{K}(k_f)}{\mathrm{K}(k_f')}. \quad (11)$$

Therefore, the effective relative permittivity and characteristic impedance are

$$\varepsilon_{\mathrm{eff}} = C/C_0 = 1 + (\varepsilon_{r1} - 1)q_1 + (\varepsilon_{r2} - 1)q_2 \quad (12)$$

and

$$Z_0 = \frac{120\pi\varepsilon_0}{C_0\sqrt{\varepsilon_{\mathrm{eff}}}} = \frac{120\pi}{\left(\mathrm{K}(k_i)/\mathrm{K}(k_i') + \mathrm{K}(k_b)/\mathrm{K}(k_b')\right)\sqrt{\varepsilon_{\mathrm{eff}}}}, \quad (13)$$

where the filling factors q_1 and q_2 are expressed as

$$q_1 = \frac{\mathrm{K}(k_b)/\mathrm{K}(k_b')}{\mathrm{K}(k_i)/\mathrm{K}(k_i') + \mathrm{K}(k_b)/\mathrm{K}(k_b')} \quad (14)$$

and

$$q_2 = \frac{\mathrm{K}(k_f)/\mathrm{K}(k_f')}{\mathrm{K}(k_i)/\mathrm{K}(k_i') + \mathrm{K}(k_b)/\mathrm{K}(k_b')}. \quad (15)$$

It should be noted that various multilayered ACPWs with or without upper shielding and conductor backing can be analyzed with the foregoing methods. Furthermore, when the required characteristic impedance Z_0 and the supplied substrates (ε_{r1}, ε_{r2}, h_1, h_2) are given, the physical dimensions of the ACPWCBSO cannot be directly obtained from the foregoing formulas. To solve this problem, the ANNs will be used in section IV to construct the synthesis models to directly obtain the physical dimensions of the ACPWCBSO.

III. ANN Trained with Modified GA-LM Algorithm

An important class of ANNs is the multilayer perceptron (MLP) [18], which is suitable for modeling high-dimensional and highly nonlinear problems. Therefore, it has been widely used to construct the analysis and synthesis models for various microwave transmission lines [18]-[20]. It is found in [18]-[20] that for thousands of samples with different electrical properties and geometrical dimensions, the existing GA-LM algorithm [23], [25] and the LM algorithm [26] can make both the MSE and the average relative error (ARE) of the MLP small. However, the MRE may be greater than 15%. This will be proven in section V. To solve this problem, a modified GA-LM algorithm is presented here. In this algorithm, the MRE is used as the fitness function of the chromosomes, guaranteeing that the MRE is small, and the MSE is used as the error function in LM training, ensuring that the ARE is small. Figure 5 is the flowchart of the ANN trained with the modified GA-LM algorithm. More detailed steps are described as follows:

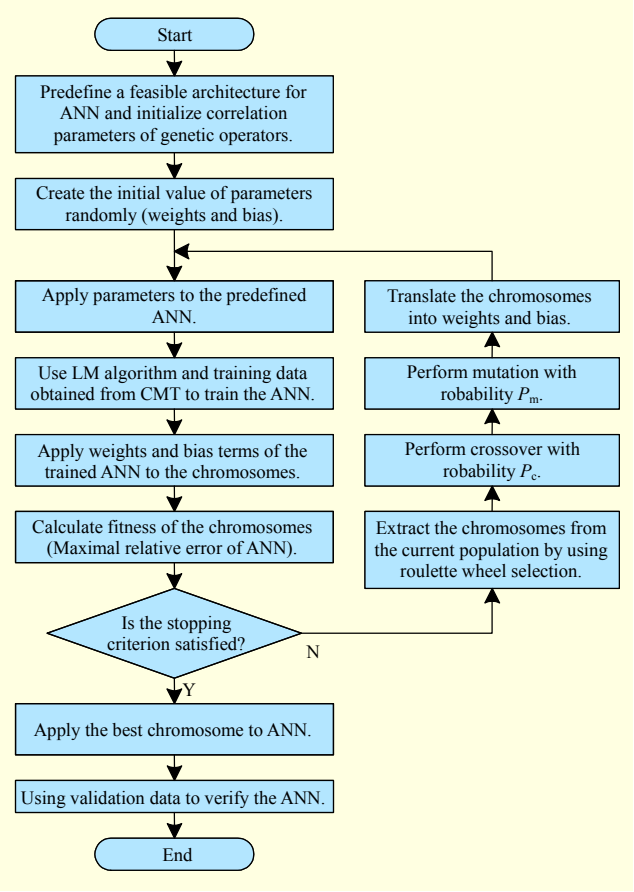

Fig. 5. Flowchart of ANN trained with modified GA-LM algorithm.

1) Predefine a feasible architecture for an ANN and initialize the correlation parameters of genetic operators, including the size of population S_{pop}, the probability of crossover and mutation (P_c and P_m), and the max generation M_{gen}.
2) Create the initial values of the ANN parameters randomly.
3) Apply the weights and bias parameters to the predefined ANN.
4) Use the LM algorithm and training data obtained from the CMT analysis to train the ANN with N_1 or N_2 epochs to reduce the MSE. Note that $N_1 > N_2$, and the training epochs N_1 is used only when initializing the population. This is because, with appropriate N_1 and N_2 epochs, the ANN training can be accelerated and the ANN will not be overtrained. In our experiments, N_1 and N_2 are set as 100 and 25, respectively.
5) Apply the weights and bias parameters of the trained ANN to the chromosomes that constitute the current population.
6) Calculate the fitness of the chromosomes. The MRE of the

ANN is used as the fitness function.

7) Estimate the stopping criterion. If the ANN does not meet the accuracy requirements and the number of current generations of the GA operation is less than M_{gen}, go to "step 8)" to implement the GA operation. Otherwise, stop the training and go to "step 10)".
8) Genetic operators, such as selection and crossover and mutation, are implemented. In this study, the roulette wheel selection is applied in the reproduction, and the probability values of crossover and mutation are set to 0.4 and 0.2, respectively.
9) Translate the chromosomes into weights and bias, and then return to "step 3)" for LM training.
10) Apply the values of the best chromosome to the ANN, and then use validation data to verify the ANN.

It should be noted that the GA-LM algorithm presented above is different from the algorithm given in [23] and [25], in which the MRE was not taken into account.

IV. ANN Synthesis Models

An ANN used to analyze microwave transmission lines can be called a "forward model," in which the model inputs are geometric parameters and the outputs are electrical parameters [17]. For the purpose of synthesis, the information is often processed in the reverse direction to find the geometric parameters for the given values of the electrical parameters, which is called the "inverse problem." Unlike the forward model, in which the input-to-output mapping is usually a one-to-one mapping, the inverse model often encounters the problem of multiple solutions [17]. This problem also causes difficulties during training because the same input values to the inverse model will lead to different values at the output. As a result, the neural network inverse model cannot be trained accurately [17]. To overcome this problem, some geometric parameters are used as the input values in our synthesis models to ensure a unique value at the output. Figure 6 illustrates the synthesis models. The synthesis model I can be used to calculate the central strip width w for the given substrates (ε_{r1}, ε_{r2}, h_1, h_2) and required characteristic impedance Z_0 by choosing the appropriate g_1 and g_2. The synthesis model II can be adopted to compute the slot width g_2 for the given substrates (ε_{r1}, ε_{r2}, h_1, h_2) and required characteristic impedance Z_0 by choosing the appropriate w and g_1/g_2.

The ANN model is a type of black box model, whose accuracy depends on the data sets used during training. To obtain the training and test data sets, (13) is used to generate data for $1 \le \varepsilon_{r1} \le 22$, $1 \le \varepsilon_{r2} \le 22$, $0.05 \le h_1/h_2 \le 10$, $0.05 \le w/h_1 \le 2$, $0.1 \le g_2/h_1 \le 2$, and $0.1 \le g_1/g_2 \le 1$. The selection of training parameters mostly depends on experience with the problem. In this study, the training data sets for the synthesis models are selected in accordance with the ranges of characteristic impedance $20\ \Omega \le Z_0 \le 70\ \Omega$ and $70\ \Omega \le Z_0 \le 210\ \Omega$. The selected data is then arranged into the input and output matrices. For the synthesis model I, a six-row matrix [ε_{r1}, ε_{r2}, h_1/h_2, g_2/h_1, g_1/g_2, Z_0] is used as the input matrix; a single-row matrix containing the corresponding values of w/h_1 is used as the output matrix. Similarly, the six-row matrix [ε_{r1}, ε_{r2}, h_1/h_2, w/h_1, g_1/g_2, Z_0] and single-row matrix [g_2/h_1] are respectively used as the input matrix and the output matrix for the synthesis model II. To facilitate an easier learning process, the elements of each row of the input and output matrices are scaled with respect to the row minimum and maximum values (for example, 1 and 22 for the row, including relative permittivity ε_{r1}) to transform their range to [–1, 1] before training. Lastly, out of the 10,000 data sets generated for each ANN synthesis model, 7,000 are used for training and the rest are used to test the trained model.

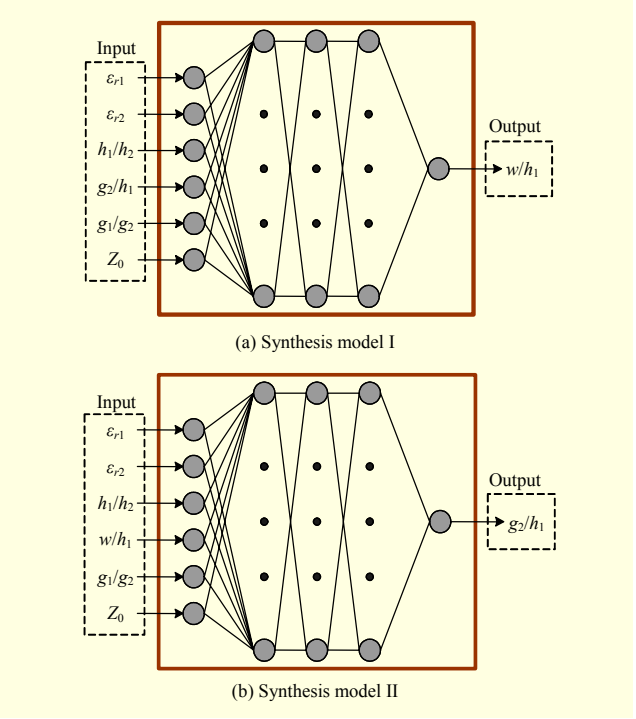

Fig. 6. ANN synthesis models for ACPWCBSO.

For the neural network to be an accurate synthesis model of the microwave transmission lines, a suitable number of hidden neurons are needed. The number of hidden neurons depends upon the degree of nonlinearity of the input-to-output mapping and the dimensionality of the input and output matrices. Highly nonlinear mappings need more neurons, while smoother items need fewer neurons. However, the universal approximation theorem does not specify what size the MLP network should be. The precise number of hidden neurons required for a given modeling task remains an open question [17]. Designers can

Table 1. Network configuration for ANN synthesis models.

Characteristic impedance	Synthesis model I	Synthesis model II
$20\ \Omega \le Z_0 \le 70\ \Omega$	6×30×60×30×1	6×30×60×30×1
$70\ \Omega \le Z_0 \le 210\ \Omega$	6×30×60×5×1	6×30×60×30×1

Table 2. Comparison of ANN synthesis model I with different network configuration for $70\ \Omega \le Z_0 \le 210\ \Omega$.

Network configuration	Training		Test		Training time (s)
	MRE (%)	ARE (‰)	MRE (%)	ARE (‰)	
6×30×80×1	3.71	1.90	15.3	3.30	9,014
6×30×70×1	3.06	1.96	18.5	3.29	7,884
6×30×60×1	28.1	9.17	28.1	10.4	6,274
6×30×60×5×1	1.00	0.51	8.05	1.09	6,085
6×30×60×10×1	1.73	0.89	8.27	1.57	8,461

use either experience or a trial-and-error process to judge the number of hidden neurons. In general, the MLPs with two or three hidden layers are commonly used to construct the analysis and synthesis models for microwave transmission lines [18]-[20].

To obtain accurate synthesis models for the ACPWCBSO, many experiments are conducted in this study. After many trials, the suitable network configuration for the first synthesis model is 6×30×60×30×1, which means that the number of neurons is 6, 30, 60, 30, and 1 for the input layer, the first, second, and third hidden layers, and the output layer, respectively. The network configuration for synthesis model II is given in Table 1. For each ANN model, the tangent sigmoid activation function is used in the hidden layers, and the linear activation function is used in the output layers.

To provide more information about the selection of the network configuration, Table 2 gives the comparison of the ANN synthesis model I with different network configurations for $70\ \Omega \le Z_0 \le 210\ \Omega$. It is observed that a network with three hidden layers is more accurate than a network with two hidden layers, and the synthesis model with a suitable network configuration (6×30×60×5×1) has the highest training efficiency. Furthermore, more hidden neurons require more training time when the number of hidden layers is the same.

V. Experiment Results and Discussion

In this study, ANNs are successfully adapted for the synthesis of the ACPWCBSO. They are trained with the modified GA-LM algorithm, the existing GA-LM algorithm [25], and the LM algorithm [26]. The learning epoch for the LM algorithm is 300. The max generation of the GA operation M_{gen} and the size of the population S_{pop} are respectively set up to be 8 and 6 in the GA-LM algorithm, and the corresponding learning epoch for each chromosome is also 300. The training time for the ANN synthesis models trained with the GA-LM algorithm is about six times that when only using the LM algorithm. However, the elapsed time for the trained ANN synthesis models used to synthesize the ACPWCBSO is only about 0.1 seconds, which is independent on the training algorithms. Furthermore, based on the trained ANN synthesis models, we can program a transmission-line calculator similar to the *TX-LINE* [27] or the *LineCalc* [28], and the RF engineer does not need to spend a lot of time training ANNs. Therefore, the training time is not an obstacle to the ANN synthesis of the ACPWCBSO.

The MREs and the AREs of the ANN synthesis models trained with the modified GA-LM algorithm, the existing GA-LM algorithm [25], and the LM algorithm [26] are given in Table 3. It is observed that when using the existing GA-LM algorithm and the LM algorithm, a smaller ARE can be obtained, but the MRE may be greater than 15%, even with an ARE of 1.02‰. For each ANN synthesis model trained with the modified algorithm, the MRE is less than 8.1% and the ARE is less than 1.9‰. These error values clearly show that the synthesis models presented in this study are capable of accurately computing the physical dimensions of the ACPWCBSO.

To validate the proposed ANN synthesis models, comparisons between the results of the synthesis models trained with the modified GA-LM algorithm and the CMT analysis contours are shown graphically in Figs. 7 and 8. The figures respectively plot the ratios of geometrical dimensions w/h_1 and g_2/h_1 versus the ratios of the slot widths g_1/g_2 for various characteristic impedance values with given substrate materials. Excellent agreement between the results of the CMT analysis and the ANN synthesis models using the modified GA-LM algorithm is obtained, validating the proposed method for the synthesis of the ACPWCBSO.

When the value of dielectric relative permittivity ε_{r1} is equal to 1.0, the ACPWCBSO is usually called an ACPW with upper shielding. Similarly, when the value of dielectric relative permittivity ε_{r2} is equal to 1.0, the ACPWCBSO is identified as a conductor-backed ACPW or an ACPW with conductor backing and is symmetric if the ratio g_1/g_2 is equal to 1.0. To validate the ANN synthesis models for the particular applications, we also analyzed and synthesized symmetric and asymmetric CPWs with upper shielding or conductor backing.

In Fig. 9, the results of the ANN synthesis models are compared with the CMT analysis for symmetric and

Table 3. Errors obtained from synthesis models trained with modified GA-LM algorithm and LM algorithm.

Synthesis model		Modified GA-LM algorithm				Existing GA-LM algorithm				LM algorithm			
		Training		Test		Training		Test		Training		Test	
		MRE (%)	ARE (‰)	MRE (%)	ARE (‰)	MRE (%)	ARE (‰)	MRE (%)	ARE (‰)	MRE (%)	ARE (‰)	MRE (%)	ARE (‰)
I	20 Ω≤Z_0≤70 Ω	3.78	0.86	4.23	1.34	0.64	0.20	9.51	0.65	2.74	0.60	15.1	1.34
	70 Ω≤Z_0≤210 Ω	1.00	0.51	8.05	1.09	2.03	1.10	15.2	2.08	2.02	0.89	17.0	1.38
II	20 Ω≤Z_0≤70 Ω	2.43	1.00	5.94	1.89	2.86	1.11	8.16	2.00	2.17	0.92	16.8	2.11
	70 Ω≤Z_0≤210 Ω	0.54	0.23	7.23	0.66	0.62	0.21	10.7	0.73	0.28	0.13	17.3	1.02

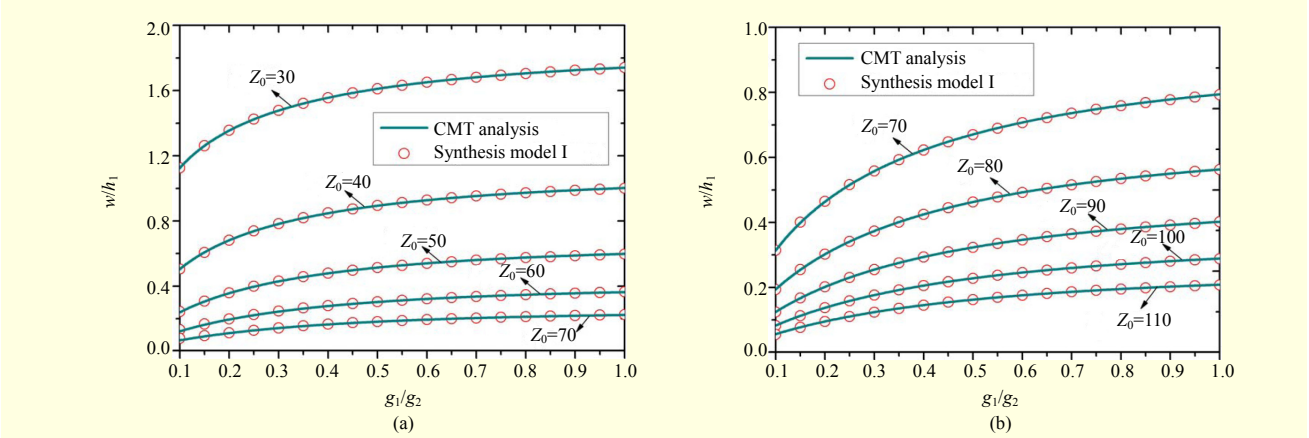

Fig. 7. Comparison of results obtained from ANN synthesis model I trained with modified GA-LM algorithm and CMT analysis contours for ACPWCBSO: (a) required characteristic impedance among 20 Ω ≤ Z_0 ≤ 70 Ω (ε_{r1}=12.9, ε_{r2}=2.65, h_1=250 μm, h_2=750 μm, and g_2/h_1=1) and (b) required characteristic impedance among 70 Ω ≤ Z_0 ≤ 210 Ω (ε_{r1}=4.3, ε_{r2}=2.65, h_1=1,000 μm, h_2=1,000 μm, and g_2/h_1=1).

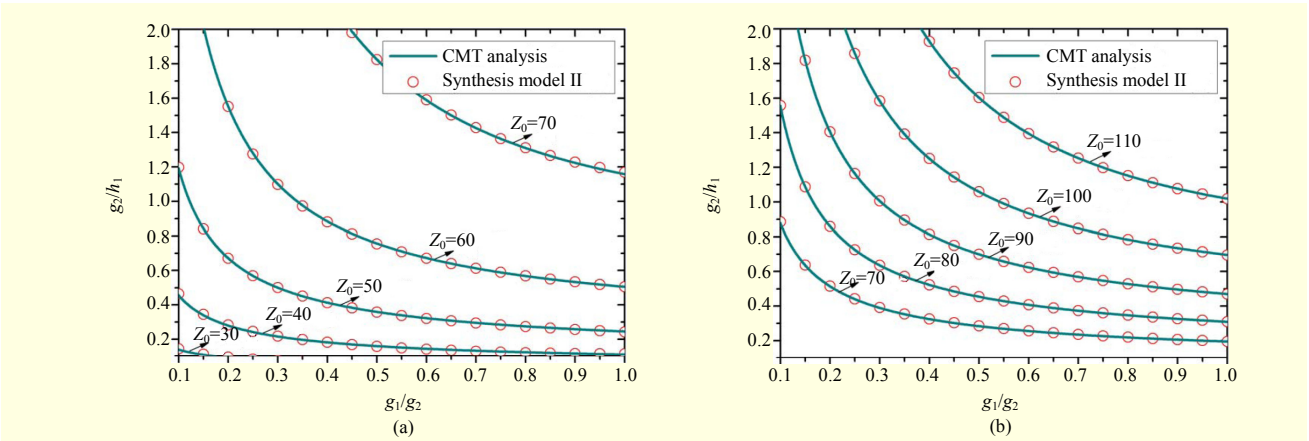

Fig. 8. Comparison of results obtained from ANN synthesis model II trained with modified GA-LM algorithm and CMT analysis contours for ACPWCBSO: (a) required characteristic impedance among 20 Ω ≤ Z_0 ≤ 70 Ω (ε_{r1}=12.9, ε_{r2}=6.15, h_1=1,000 μm, h_2=500 μm, and w/h_1=0.2) and (b) required characteristic impedance among 70 Ω ≤ Z_0 ≤ 210 Ω (ε_{r1}=2.65, ε_{r2}=6.15, h_1=1,000 μm, h_2=500 μm, and w/h_1=0.2).

asymmetric CPWs with upper shielding (ε_{r1}=1, ε_{r2}=12.9, h_1=1,500 μm, h_2=500 μm, and g_2/h_2=1.5). The characteristic impedances are plotted with respect to the ratio of geometrical dimensions w/h_2 for three different g_1/g_2 values. The

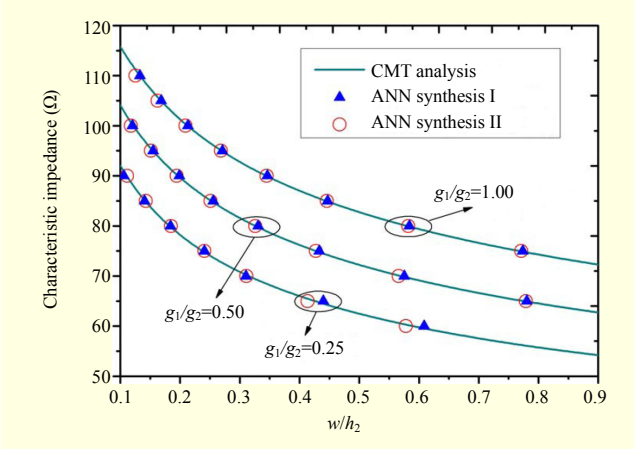

Fig. 9. Comparisons of results of ANN synthesis models presented in this study and CMT analysis for symmetric and asymmetric CPWs with upper shielding (ε_{r1}=1, ε_{r2}=12.9, h_1=1,500 μm, h_2=500 μm, and g_2/h_2=1.5).

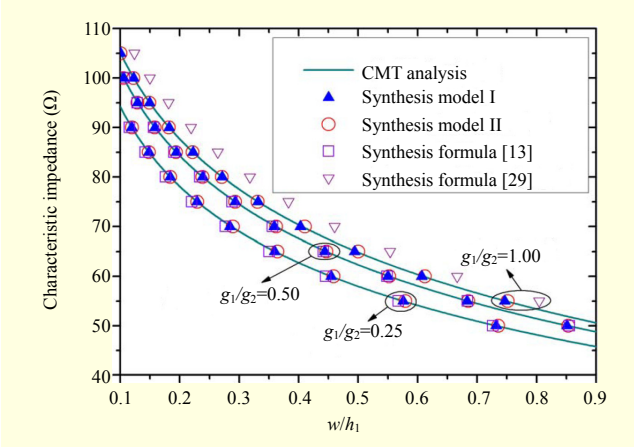

Fig. 10. Comparisons of results of ANN synthesis models, synthesis formulas [13], [29], and CMT analysis for symmetric and asymmetric CPWs with conductor backing (ε_{r1}=10.2, h_1=1,270 μm, and g_2/h_1=1.5).

comparisons among the results of the ANN synthesis models in the study, the synthesis formulas [13], [29], and the CMT analysis for symmetric and asymmetric CPWs with conductor backing (ε_{r1}=10.2, h_1=1,270 μm, and g_2/h_1=1.5) are shown in Fig. 10. It is observed that the results of the proposed ANN synthesis models for asymmetric CPWs with conductor backing are in agreement with the results of the synthesis formulas given in [13], and the accuracy of the proposed ANN synthesis models for symmetric CPWs with conductor backing is higher than that of the synthesis formulas presented in [29]. As clearly seen from Figs. 9 and 10, there is a self-consistent agreement between the ANN synthesis models presented in this study. It is also apparent from the figures that there is excellent agreement among the results obtained from the proposed ANN synthesis models and the CMT analysis for asymmetric and symmetric CPWs with upper shielding or conductor-backing.

In Table 4, the results obtained from the ANN synthesis models trained with the modified GA-LM algorithm are compared with the results of the CMT analysis, the synthesis formulas [13], [29], HFSS electromagnetic simulation [30], and experimental work [13]. The measured characteristic impedance with geometrical dimensions w, g_1, and g_2 is represented by Z_{0m}, while the characteristic impedance values obtained from the HFSS and the CMT analysis using w, g_1, and g_2 are represented by Z_{0h}, and Z_{0c}, respectively. In Table 4, w_I and w_f represent the strip width obtained from the proposed ANN synthesis model I and the synthesis formulas [13], [29] using Z_{0c}, g_1, and g_2. Finally, the CMT analysis results (Z_{0I} and Z_{0f}) are calculated using w_I and w_f for checking. Similar results of the proposed ANN synthesis model II are omitted here for conciseness. From Table 4, the relative error of physical dimensions obtained from the ANN-based model I is less than 0.4%, which is smaller than that of the synthesis formulas [13], [29]. An agreement is obtained between the theoretical and experiment results.

VI. Conclusion

In this paper, two ANN synthesis models trained with a modified GA-LM algorithm were presented for the

Table 4. Comparisons of results of proposed ANN synthesis models, CMT, HFSS, synthesis formulas [13], [29], and experiment results.

Substrate materials		Measured				HFSS	CMT	ANN synthesis model I		Synthesis formulas [13], [29]		Relative error	
ε_{r1}	h_1 (μm)	w (μm)	g_1 (μm)	g_2 (μm)	Z_{0m} (Ω)	Z_{0h} (Ω)	Z_{0c} (Ω)	w_I (μm)	Z_{0I} (Ω)	w_f (μm)	Z_{0f} (Ω)	$\lvert w_I\text{-}w\rvert/w$ (%)	$\lvert w_f\text{-}w\rvert/w$ (%)
10.2	1,270	1,050	1,100	1,100	49.73	49.35	49.93	1,047	49.99	1,027	50.42	0.29	2.19
		800	300	1,400	47.89	48.78	49.52	802	49.46	802	49.47	0.25	0.29
9.9	800	800	400	400	40.03	41.96	42.88	797	42.94	753	44.06	0.38	5.88
		800	400	800	42.14	43.72	44.87	800	44.86	808	44.66	0	1.00

ACPWCBSO. The ANN synthesis models were verified by comparing their results with the results of the CMT analysis, HFSS simulation, and measurements. The MRE and ARE of the ANN synthesis models were calculated. For each model trained with the modified GA-LM algorithm, the MRE was less than 8.1% and the ARE was less than 1.9%. These error values clearly show that the ANN synthesis models trained with the modified GA-LM algorithm can be used to accurately compute the physical dimensions of the ACPWCBSO simply, rather than by the iteration technique of applying the analysis methods (CMT or HFSS). In addition, the models can be used for both symmetric and asymmetric CPWs with conductor backing or upper shielding.

References

[1] R.N. Simons, *Coplanar Waveguide Circuits, Components, and Systems*, New York: Wiley-IEEE Press, 2001.

[2] D. Chang, B. Zeng, and J. Liu, "CPW-Fed Circular Fractal Slot Antenna Design for Dual-Band Applications," *IEEE Trans. Antennas Propag.*, vol. 56, no. 12, Dec. 2008, pp. 3630-3636.

[3] T. Jang and S. Lim, "A Compact Zeroth-Order Resonant Antenna on Vialess CPW Single Layer," *ETRI J.*, vol. 32, no. 3, Jun. 2010, pp. 472-474.

[4] V.F. Hanna and D. Thebault, "Theoretical and Experimental Investigation of Asymmetric Coplanar Waveguides," *IEEE Trans. Microw. Theory Tech.*, vol. 32, no. 12, Dec. 1984, pp. 1649-1651.

[5] J.J. Chang and W.S. Wang, "Characteristics of Asymmetrical Conductor-Backed Coplanar Waveguides," *Int. J. Electron.*, vol. 72, no. 4, Apr. 1992, pp. 641-650.

[6] Z.B. Wang et al., "A Broadband 3 dB Coplanar Waveguides Directional Coupler with Conductor-backed Asymmetric Coplanar Waveguides Compensation," *IETE J. Res.*, vol. 58, no. 1, Jan.-Feb. 2012, pp. 72-76.

[7] A.M. Peláez-Pérez et al., "Ultra-Broadband Directional Couplers Using Microstrip with Dielectric Overlay in Millimeter-Wave Band," *Prog. Electromagn. Res.*, vol. 117, 2011, pp. 495-509.

[8] Z.B. Wang et al., "An Inmarsat BGAN Terminal Patch Antenna Array with Unequal Input Impedance Elements and Conductor-Backed ACPW Series-Feed Network," *IEEE Trans. Antennas Propag.*, vol. 60, no. 3, Mar. 2012, pp. 1642-1647.

[9] C. Karpuz et al., "Fast and Simple Analytical Expressions for Quasistatic Parameters of Asymmetric Coplanar Lines," *Microw. Opt. Technol. Lett.*, vol. 9, no. 6, Aug. 1995, pp. 334-336.

[10] A. Görür, C. Karpuz, and M. Alkan, "Quasistatic TEM Characteristics of Overlayed Supported Asymmetric Coplanar Waveguides," *Int. J. Microwave. Millimeter. Wave. Comput. Aided. Eng.*, vol. 6, no. 5, Sep. 1996, pp. 297-304.

[11] C. Karpuz and A. Görür, "Effect of Upper Shielding and Conductor Backing on Quasistatic Parameters of Asymmetric Coplanar Waveguides," *Int. J. RF Microwave. Comput. Aided. Eng.*, vol. 9, no. 5, Sep. 1999, pp. 394-402.

[12] S.J. Fang and B.S. Wang, "Analysis of Asymmetric Coplanar Waveguide with Conductor Backing," *IEEE Trans. Microw. Theory Tech.*, vol. 47, no. 2, Feb. 1999, pp. 238-240.

[13] S. Kaya et al., "New and Accurate Synthesis Formulas for Asymmetric Conductor-Backed Coplanar Waveguides," *Microw. Opt. Technol. Lett.*, vol. 53, no. 1, Jan. 2011, pp. 211-216.

[14] S. Kaya and K. Guney, "New and Accurate Synthesis Formulas for Asymmetric Coplanar Waveguides," *Microw. Opt. Technol. Lett.*, vol. 53, no. 9, Sep. 2011, pp. 1991-1996.

[15] Q.J. Zhang and K.C. Gupta, *Neural Networks for RF and Microwave Design*, Boston: Artech House Publishers, 2000.

[16] Q.J. Zhang, K.C. Gupta, and V.K. Devabhaktuni, "Artificial Neural Networks for RF and Microwave Design—From Theory to Practice," *IEEE Trans. Microw. Theory Tech.*, vol. 51, no. 4, Apr. 2003, pp. 1339-1350.

[17] H. Kabir et al., "Smart Modeling of Microwave Devices," *IEEE Microwave Mag.*, vol. 11, no. 3, May 2010, pp. 105-118.

[18] E.D. Übeyli and İ. Güler, "Multilayer Perceptron Neural Networks to Compute Quasistatic Parameters of Asymmetric Coplanar Waveguides," *Neurocomputing*, vol. 62, no. 1-4, Dec. 2004, pp. 349-365.

[19] C. Yildiz et al., "Neural Models for Coplanar Strip Line Synthesis," *Prog. Electromagn. Res.*, vol. 69, 2007, pp. 127-144.

[20] P.T. Selvan and S. Raghavan, "Neural Model for Circular-Shaped Microshield and Conductor-Backed Coplanar Waveguide," *Prog. Electromagn. Res. M*, vol. 8, 2009, pp. 119-129.

[21] V.P. Plagianakos, G.D. Magoulas, and M.N. Vrahatis, "Learning in Multilayer Perceptrons Using Global Optimization Strategies," *Nonlinear Anal. Theory Methods Appl.*, vol. 47, no. 5, Aug. 2001, pp. 3431-3436.

[22] R.K. Belew, J. McInerey, and N.N. Schraudolph, "Evolving Networks: Using the Genetic Algorithm with Connectionist Learning," University of California, Tech. Rep. CS90-174, 1990.

[23] R.B.C. Prudêncio and T.B. Ludermir, "Neural Network Hybrid Learning: Genetic Algorithms & Levenberg-Marquardt," *Proc. 26th Annu. Conf. Gesellschaft for Classification*, 2003, pp. 464-472.

[24] Y. Kim et al., "Application of Artificial Neural Networks to Broadband Antenna Design Based on a Parametric Frequency Model," *IEEE Trans. Antennas Propag.*, vol. 55, no. 3, Mar. 2007, pp. 669-674.

[25] C. Zhang et al., "A Novel GA-LM Based Hybrid Algorithm," *Proc. ICNC*, 2007, pp. 479-483.

[26] M.T. Hagan and M.B. Menhaj, "Training Feedforward Networks with the Marquardt Algorithm," *IEEE Trans. Neural Netw.*, vol. 5, no. 6, Nov. 1994, pp. 989-993.

[27] http://web.awrcorp.com/Usa/Products/Optional-Products/TX-Line/

[28] http://newport.eecs.uci.edu/eceware/ads_docs/pdf/linecalc.pdf

[29] C. Yildiz and M. Turkmen, "Synthesis Formulas for Conductor-Backed Coplanar Waveguide," *Microw. Opt. Technol. Lett.*, vol. 50, no. 4, Apr. 2008, pp. 1115-1117.
[30] *Ansoft High Frequency Structure Simulator (HFSS)*, Ver. 11.0, Ansoft Corporation.

Zhongbao Wang received his BEng and MEng in communication engineering from Dalian Maritime University (DLMU), Liaoning, China, in 2007 and 2009, respectively, and is currently working toward his PhD at DLMU. His current research interests include patch antennas, passive RF components, and microwave technology using artificial intelligence. He was the recipient of the Best Master's Thesis Award of Liaoning Province in 2009.

Shaojun Fang received his PhD in communication and information systems from Dalian Maritime University (DLMU), Liaoning, China, in 2001. Since 1982, he has been working at DLMU, where he is currently a head professor in the School of Information Science and Technology. His recent research interests include patch antennas and computational electromagnetics. He has authored or coauthored three books and over 80 journal and conference papers. He was the recipient of the Best Doctor's Dissertation Award of Liaoning Province in 2002 and the Outstanding Teacher Award of the Ministry of Transport of China.

Shiqiang Fu received his PhD in communication and information systems from Dalian Maritime University (DLMU), Liaoning, China, in 2010. He is currently a lecturer in the School of Information Science and Technology, DLMU. His current research interests include passive RF components and satellite mobile terminal antennas for INMARSAT.